Regulation of murine hematopoietic stem cell quiescence by Dmtf1

Michihiro Kobayashi[1] and Edward F. Srour[1-3]

Departments of [1]Medicine, [2]Pediatrics, and [3]Microbiology and Immunology, Indiana University School of Medicine, Indianapolis, IN

The cell-cycle status of hematopoietic stem cells (HSCs) is tightly regulated, most likely to balance maintenance of stem-cell status through quiescence and expansion/differentiation of the hematopoietic system. Tumor-suppressor genes (TSGs), with their cell cycle–regulatory functions, play important roles in HSC regulation. The cyclin-D binding myb-like transcription factor 1 (Dmtf1) was recently recognized as a TSG involved in human cancers by repressing oncogenic Ras/Raf signaling. However, the role of Dmtf1 in the hematopoietic system is entirely unknown. In the present study, we demonstrate that Dmtf1 regulates HSC function under both steady-state and stress conditions. *Dmtf1*$^{-/-}$ mice showed increased blood cell counts in multiple parameters, and their progenitor cells had increased proliferation and accelerated cell-cycle progression. In addition, long-term HSCs from *Dmtf1*$^{-/-}$ mice had a higher self-renewal capacity that was clearly demonstrated in secondary recipients in serial transplantation studies. Dmtf1$^{-/-}$ BM cells showed hyper proliferation after 5-fluorouracil–induced myeloablation. Steady-state expression and Induction of CDKN1a (p21) and Arf were impaired in HSCs from *Dmtf1*$^{-/-}$ mice. The function of Dmtf1 was mediated by both Arf-dependent and Arf-independent pathways. Our results implicate Dmtf1 in the regulation of HSC function through novel cell cycle–regulatory mechanisms. (*Blood*. 2011;118(25):6562-6571)

Introduction

Hematopoietic stem cells (HSCs) sustain hematopoiesis through a delicate balance between self-renewal and differentiation to ensure continued and life-long production of mature cells and maintenance of the stem-cell pool. These 2 functions are critically affected by the mitotic quiescence of HSCs, which is likely controlled by HSC-intrinsic mechanisms and BM microenvironmental factors.[1] Tumor-suppressor genes (TSGs) that negatively influence cell-cycle regulation have been widely investigated for their role in HSC function. Early studies suggested a role for Cdkn1a (p21) in regulating HSC pool size and HSC exhaustion under stress.[2] More recent studies, however, concluded that the role of Cdkn1a (p21) in regulating HSC self-renewal was minimal.[3,4] Similarly, other cyclin-dependent kinase inhibitors, including Cdkn1b (p27)[5] and Cdkn2b (p15),[6] do not have critical roles in HSC self-renewal, although Cdkn2c (p18) maintains this property.[7] Because the p19^{Arf} (Arf) and p16^{Ink4a} (Ink4a) are independent gene products derived from a shared Arf/Ink4a genetic locus and are involved in the p53 and Rb pathways, respectively, they are frequently disrupted in human cancers.[8] *Arf*-deficient mice and mice with mutations in the common *Arf/Ink4a* locus do not have a critical HSC phenotype during proliferative stress.[9] However, functional deficiency of *Bmi1*-null HSCs is dramatically compensated for by disruption of *Arf/Ink4a*,[10] indicating that these molecules are important for HSC self-renewal in specific situations. Deletion of *Pten* leads to depletion of the HSC pool over time, showing its prominence in maintaining stem cells.[11] The adenomatous polyposis coli TSG is critical for HSC maintenance because its conditional deletion results in rapid HSC exhaustion.[12] The p53 TSG may regulate various aspects of HSC behavior.[13-16] Al-though hematopoiesis in *p53*-knockout (*p53*-KO) mice appears to proceed normally, numerous studies have identified roles for p53 in the proliferation, differentiation, apoptosis, and aging of hematopoietic cells[17-19] and the regulation of HSC quiescence.[20]

Recently, cyclin D binding myb-like transcription factor-1 (Dmtf1), also known as cyclin D binding myb-like protein-1 (Dmp1), has been recognized as a TSG involved in negatively regulating cell-cycle progression mainly through an Arf-Mdm2-p53–dependent mechanism.[21-23] Dmtf1 binds directly to the Arf promoter to activate its expression, thereby inducing a p53-dependent cell-cycle arrest.[24] Both *Dmtf1*-null and heterozygote (Het) mice are prone to spontaneous tumor development.[22,25] Because the wild-type (WT) *Dmtf1* allele is retained and expressed in tumors arising in Het mice, Dmtf1 is haploinsufficient for tumor suppression.[25] Given that the deletion or mutation of *Arf* or *p53* is rare in tumors from *Dmtf1*$^{-/-}$ mice, Dmtf1 may be a physiologic regulator of the Arf-p53 pathway.[26] Moreover, deletion of *Dmtf1* is found in human lung cancer cells[27] and some leukemia cells.[27,28] The Dmtf1 promoter is activated by growth-promoting signals via the Ras/Raf/MEK/ERK pathway, and the induction of Arf by Ras is Dmtf1 dependent.[23] Although it is generally believed that induction of Arf is Dmtf1 dependent,[29] other targets for Dmtf1 remain unknown in hematopoietic cells, especially lymphocytes.[29]

At present, little is known about the role of Dmtf1 in HSC maintenance. Therefore, in the present study, we performed a detailed analysis of the functions of Dmtf1 in the hematopoietic system, focusing on HSC regulation, and identified novel mechanisms through which Dmtf1 participates in the maintenance of HSC quiescence.

Methods

Mice and blood counts

Dmtf1-null mice backcrossed onto C57BL/6 (B6) mice were kindly provided by Dr K. Inoue (Wake Forest University, Winston-Salem, NC). B6.SJL-PtrcAPep3B/BoyJ (BJ; CD45.1) and B6/BJ-F1 (CD45.1/CD45.2) mice were bred in-house. Null mice were used at 11-18 weeks of age. Littermates were used as controls. Mice were maintained at the Indiana University School of Medicine animal facility and all studies were approved by the institutional animal care and use committee. Peripheral blood (PB) samples were collected by tail bleeding into tubes containing EDTA. Complete blood counts and differentials were obtained using a Hemavet 950FS (Drew Scientific).

Progenitor cell assay

For CFU assays, BM mononuclear cells (BM-MNCs) and sorted cKit$^+$/Sca1$^+$/Lineage$^-$ (KSL) cells were plated in duplicate in methylcellulose medium (Methocult M3242; StemCell Technologies) supplemented with SCF (10 ng/mL), IL3 (5 ng/mL), thrombopoietin (5 ng/mL), GM-SCF (5 ng/mL), and erythropoietin (3 U/mL), and scored on day 10.

Flow cytometry

The following mAbs were used: c-Kit (2B8), Sca1 (E13-161.7), CD4 (L3T4), CD8 (53-6.7), B220 (RA3-6B2), Ter119 (Ly-76), Gr-1 (RB6-8C5), FITC-CD34 (RAM34), PE-CD16/32w (93), PE-CD135 (A2F10), PerCP-Cy5.5-CD150 (TC15-12F12.2), PE (or FITC)–CD48 (HM48-1), CD45.1 (A20), CD45.2 (104), and CD11b (M1/70). All mAbs were from BD Biosciences or eBioscience except CD150, which was from BioLegend. Lineage-positive (Lin$^+$) cells were identified by a mixture of CD3, CD4, B220, TER-119, CD11b, or Gr-1 mAbs. Flow cytometric analysis was carried out on an LSRII or FACSCalibur flow cytometer (BD Biosciences). Cell sorting was performed on a FACSVantage SE or a FACSAria cell sorter (BD Biosciences).

Cell-cycle analysis and apoptosis

Using mAbs against c-Kit, Lin, and Sca1, KSL cells were identified and then fixed/permeabilized with Cytofix/Cytoperm (BD Biosciences), and stained with Hoechst-33342 (2 μg/mL; Molecular Probes) and Pyronin-Y (4 μg/mL; Sigma-Aldrich; Hst/Py) for 20 minutes. Cell-cycle status of KSL cells was determined on an LSR II. For DAPI staining, cells were stained with KSL, CD16/32w, and CD34, fixed, and treated with DAPI solution (5 μg/mL; Molecular Probes). BM Lin$^-$ cells isolated on a MACS cell-separator system (Miltenyi Biotec) were stained with propidium iodide and annexin V–allophycocyanin (BD Biosciences) to detect apoptotic cells.

5-FU treatment and BrdU incorporation

5-Fluorouracil (5-FU; Sigma-Aldrich) was administered intraperitoneally into mice previously transplanted with 5×10^5 MNCs from WT or KO mice 3 months previously. 5-FU was administered at 135 mg/kg/wk for 3 consecutive weeks, and survival was monitored daily. For the kinetic studies of BM ablation, a single dose (150 mg/kg) of 5-FU was injected intraperitoneally and PB counts were measured every 3-4 days. For BrdU incorporation, mice received an IP injection of 120 mg/kg of BrdU (Sigma-Aldrich) at day 5 after 5-FU treatment. BM cells were collected 2 hours after BrdU injection. MNCs were stained for KSL, CD150, and CD48, followed by staining with anti-BrdU–Alexa Fluor 647 (Invitrogen) according to the manufacturer's directions.

BM transplantation

Lethally irradiated (11 Gy split-dose > 3 hours apart) 8-week-old B6/BJ-F1 mice were reconstituted with BM-MNCs, KSL cells, or CD34$^-$135$^-$KSL cells from *Dmtf1*$^{+/+}$ or *Dmtf1*$^{-/-}$ mice (CD45.2) as described in "Results." In some studies, mice also received competitive BM-MNCs from age-matched BJ mice. Where indicated, KSL cells were cultured with cytokines (SCF, thrombopoietin, IL-3, and Flt-3 ligand) for 72 hours before transplantation. Reconstitution was monitored by flow cytometric analysis with CD45.2, CD45.1, CD3, B220, and Gr-1. For serial transplantation, BM cells (2-3 × 10^6) from primary recipients at 16 weeks after transplantation were transplanted into lethally irradiated secondary mice.

Expression vectors and retroviral production

The MSCV-IRES-GFP (MIG) plasmid containing full-length mouse Arf was kindly provided by Dr K. Inoue (Wake Forest University, Winston-Salem, NC). Empty vector (MIG-Mock) or MIG-Arf were transfected into Phoenix Eco cells using Turbofect (Fermentas) according to the manufacturer's instructions. Retrovirus transduction into mouse BM cells was performed as described previously.[30] Green fluorescent protein–positive (GFP$^+$) cells were sorted 48-72 hours after infection and used in the CFU assays. Human full-length (FL) Dmtf1 cDNA was amplified by RT-PCR from total RNA from human BM cells with the primers 5-TGTAGCTGATCCATCCGT-TGT-3 and 5-GGGGTTGCTCCTATTTCTTTG-3, and cloned into pDrive cloning vector (QIAGEN). To make the dominant negative (DN) form of hDmtf1 lacking the myb-homology repeat (MHR) domain, the downstream fragment from the MHR domain was amplified and cloned into pDrive with the primers 5-_ACCGGT_GGACCATCAAAAGGCAAA-3 (AgeI site underlined) and the same 3′ primer used for FL followed by ligation between the pDrive-FL treated with BspEI (unique site just upstream of MHR), *Xho*I (unique site in 3′), and the AgeI/*Xho*I-digested fragment. MIEG3 vector containing internal ribosome entry site–enhanced green fluorescent protein (IRES-EGFP) was obtained from Dr S. Fukuda (Indiana University, Bloomington, IN). FL or DN cDNAs were cloned into MIEG3. Amphotropic retrovirus containing FL and DN were produced using Phoenix Ampho cells (ATCC) and infected into Jurkat T cells. Transduced cells were purified by GFP sorting.

Quantitative real-time PCR

Different groups of cells from 3- to 4-month-old *Dmtf1*$^{+/+}$ and Dmtf1$^{-/-}$ mice were analyzed for the expression of Dmtf1 and other candidate genes. mRNA collection and cDNA synthesis were performed using a one-step cDNA kit (Miltenyi Biotec) following the manufacturer's instructions. RNA content was determined by SYBR Green–based real-time RT-PCR using an ABI 7500 (Applied Biosystems). Gene-expression levels were normalized to GAPDH in reference samples. Primer sequences are listed in supplemental Table 1 (available on the *Blood* Web site; see the Supplemental Materials link at the top of the online article).

Statistics

HSC function after 5-FU treatment was determined by Kaplan-Meier survival analysis and a log-rank test. The Student *t* test was used for all other analyses.

Results

Dmtf1 is expressed in HSCs and hematopoietic progenitor cells

Dmtf1, measured by quantitative RT-PCR, was expressed in various classes of hematopoietic cells, including KSL cells (supplemental Figure 1 left panel) and their subfractions. The highest expression of Dmtf1 was observed in phenotypically defined long-term HSCs (LT-HSCs; CD34$^-$CD135$^-$KSL) with lower expression in short-term HSCs (ST-HSCs; CD34$^+$CD135$^-$KSL) and multipotent progenitor (MPP) cells (CD34$^+$CD135$^+$KSL; supplemental Figure 1 right panel).

Loss of Dmtf1 alters steady-state hematopoiesis

Because growth of *Dmtf1*$^{-/-}$ mice is retarded,[22] we examined their growth pattern in detail. The body weights of 13-week-old KO male mice were significantly lower than those of their WT

Table 1. Hematopoietic parameters and organ weight in *Dmtf1*-mutant mice

	WT	KO	Het
PB count at 13 wk of age, /μL			
WBCs	16 829 ± 6338	21 418 ± 7365	16 826 ± 5163
Neutrophils	4211 ± 1672	4593 ± 2906	3647 ± 1366
Lymphocytes	11 617 ± 4679***	15 160 ± 4647###	11 957 ± 3938
Monocytes	777 ± 427**	1327 ± 552##	964 ± 419
RBCs, × 10^4/μL	114 ± 9.1*	129 ± 13.3#	115 ± 7.3
Hemoglobin, g/dL	15.8 ± 1.9*	18.7 ± 1.6#	16.3 ± 1.2
Hematocrit, %	51.3 ± 4.2*	58.9 ± 6.8#	51.7 ± 3.1
Platelets, × 10^4/μL	997.6 ± 292.1	1018.8 ± 138.2	1052.1 ± 222.3
Distribution of WBCs, %			
CD4	20.9 ± 4.94***	16.2 ± 3.71	18.4 ± 5.51
CD8	15.6 ± 3.34***	12.6 ± 2.97	13.4 ± 3.09
B220	41.6 ± 9.19	45.7 ± 8.51	43.9 ± 9.99
Myeloid	21.6 ± 4.94	24.6 ± 4.52	22.1 ± 5.98
BM count at 13 wk of age, × 10$^{7/2}$ femurs	4.94 ± 0.9*	6.75 ± 0.8#	5.35 ± 0.6
Myeloid, %	80.81 ± 7.23	74.25 ± 6.50	
B220, %	13.28 ± 4.11**	20.03 ± 3.61	
CD3, %	2.01 ± 0.57	2.18 ± 0.65	
Weights			
Body weight at 13 wk of age, g	27.9 ± 1.8*	24.5 ± 1.1#	27.5 ± 2.1
Spleen weight at 14 wk of age, mg	98.4 ± 16.1	88.4 ± 15.4	92.1 ± 14.5
Thymus weight at 14 wk of age, mg	59.6 ± 9.4*	34.8 ± 9.5#	56.3 ± 12.7

Values shown are the means ± SD (all male). PB counts are for 18-20 mice per genotype; BM cell counts are for 10-14 mice per genotype; body weights are for 10-15 mice per genotype; and spleen/thymus weights are for 7-9 mice per genotype.

* and # indicate significant statistical differences between WT and KO and KO and Het, respectively. */#$P <$ .01, **/##$P <$ .03, and ***/###$P <$ .05.

counterparts (Table 1). Consistent with the reduced number of thymocytes in KO mice ($10.8 \pm 2.65 \times 10^7$ vs $6.75 \pm 1.86 \times 10^7$ $P <$ .05, n = 4), the weight of the thymus in these mice was lower than that of WT mice. To investigate the effect of *Dmtf1* loss on steady-state hematopoiesis, we examined multiple parameters in the PB and BM of 3-month-old *Dmtf1*$^{+/+}$, *Dmtf1*$^{+/-}$, and *Dmtf1*$^{-/-}$ mice. The number of RBCs and the hemoglobin and hematocrit were increased in KO mice (Table 1), as well as the numbers of monocytes and lymphocytes. Frequencies of circulating CD4 and CD8 T cells were modestly decreased in KO mice, which is consistent with a smaller thymus (Table 1). The number of total nucleated cells in 2 femurs and the frequency of B cells in the BM of KO mice were significantly higher than in that of WT mice (Table 1).

We also investigated the progenitor-cell content of BM. The total number of CFUs was significantly higher in KO BM-MNCs and purified KSL cells compared with WT (Figure 1A-B). Interestingly, Het BM cells showed a comparable increase in the number of progenitors similar to that observed with KO BM cells (Figure 1A-B), which is consistent with functional haploinsufficiency.[25] Frequencies of phenotypically defined LT-HSCs, as determined by 2 distinct methods, CD34$^-$CD135$^-$KSL and CD48$^-$CD150$^+$KSL (slamKSL), were similar in all 3 genotypes, so the absolute numbers of these cells were comparable (Figure 1C-D and F). The absolute numbers of the most purified group of LT-HSCs as defined by Wilson et al were similar in all genotypes (Figure 1F).[31] Interestingly, the frequency of KSL cells was modestly higher in KO versus WT BM (0.19% ± 0.05% vs 0.14% ± 0.04%; Figure 1C). This increased frequency translated to a significant difference in total KSL and MPP cells (Figure 1D). Similarly, c-Kit$^+$ and Sca1$^+$ cells were significantly higher in KO mice compared with WT (Figure 1G). These data demonstrate that loss of Dmtf1 leads to a significant increase in progenitors in steady-state BM, most likely because of an increase in the number of more mature classes of progenitors in the hematopoietic hierarchy.

Differential effect of Dmtf1 on cell-cycle status of hematopoietic progenitors

Because Dmtf1 is a negative cell-cycle regulator, we evaluated its impact on the cell-cycle status of hematopoietic progenitors under steady-state hematopoiesis. The fraction of cycling cells (those in S/G$_2$ + M) among c-Kit$^+$Sca1$^-$ cells, among common myeloid progenitors (c-Kit$^+$CD34$^+$CD16/32w$^-$), and among granulocyte-macrophage progenitors (c-Kit$^+$CD34$^+$CD16/32w$^+$) was significantly higher in the BM of KO mice compared with WT mice (Figure 2A). Using Hst/Py staining to discriminate between cells in G$_0$ and G$_1$, we determined that the frequencies of cells in G$_1$ were significantly higher in KO KSL cells and reciprocally lower in G$_0$ compared with WT cells (Figure 2B). These data suggest that in steady-state, Dmtf1 increases cell-cycle progression in mature progenitors (total c-Kit$^+$ cells, common myeloid progenitors, and granulocyte-macrophage progenitors), as well as the KSL group that contains BM-repopulating cells. Because Dmtf1 is implicated in cell death,[32] we evaluated apoptosis in Lin$^-$ cells cultured with cytokines. *Dmtf1*-KO and WT Lin$^-$ cells did not differ in their kinetics of apoptosis over a period of 48 hours (Figure 2C).

Enhanced repopulating capacity of *Dmtf1*-KO LT-HSCs

We examined the BM-repopulating capacity of *Dmtf1*-KO HSCs in a competitive repopulation assay. When 2×10^5 BM-MNCs from WT or KO mice (CD45.2$^+$) were compared with an equal number of BM-MNCs from BJ mice (CD45.1$^+$) to reconstitute lethally irradiated B6/BJ-F1 recipients (CD45.2 + 45.1+), mice receiving KO MNCs achieved higher levels of chimerism than mice receiving WT MNCs at all time points analyzed (Figure 3A). At 4 months after primary transplantation, BM cells were transferred into lethally irradiated secondary B6/BJ-F1 recipients. At 3 months after transplantation, the level of engraftment of KO cells was maintained between primary and secondary recipients, whereas, as expected, that derived from WT cells
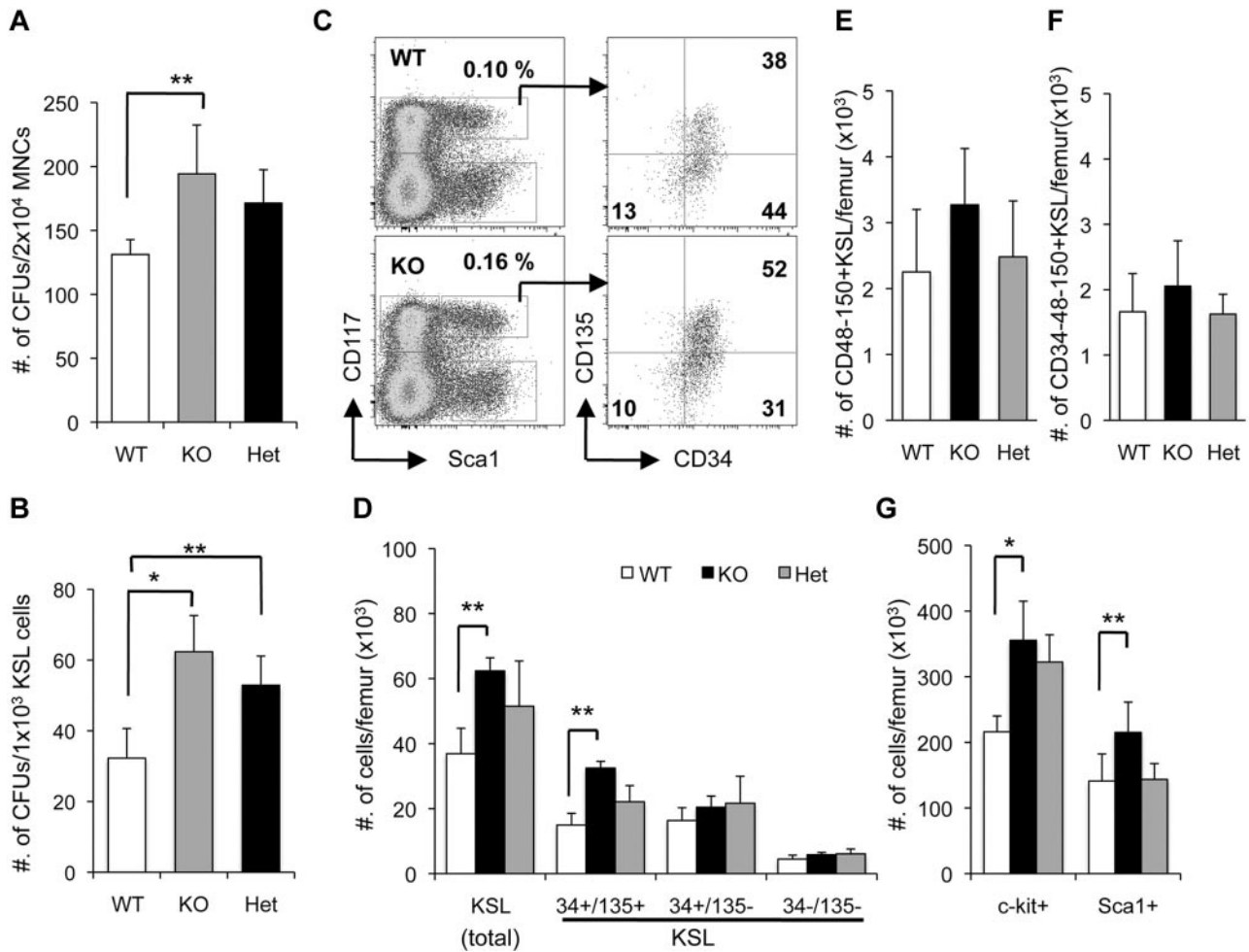
Figure 1. Enhanced proliferation of hematopoietic progenitor cells in Dmtf1−/− mice. BM-MNCs (A) or sorted KSLs (B) from WT, Dmtf1-KO, or Het mice were cultured with cytokines in methylcellulose medium for 10 days (n = 3) *P < .01 and **P < .05. (C) Representative dot plots showing MPPs (CD34+135+KSL), ST-HSCs (CD34−135−KSL), and LT-HSCs (CD34−135−KSL) in WT and Dmtf1-KO BM. (D) Quantification of the absolute number of KSLs, MPPs, ST-HSCs, and LT-HSCs and (G) quantification of the absolute number of progenitors (c-Kit+ and Sca1+) expressed as average ± SD per femur (n = 6). *P < .03 and *P < .05. (E) Absolute numbers of slamKSL (CD48−CD150+KSL) and (F) CD34− slamKSL expressed as average ± SD per femur (n = 7).

declined (Figure 3A). These data suggest that the loss of Dmtf1 may result in enhanced cell-cycle progression among primitive HSCs without premature exhaustion of their function or number. We next assayed LT-HSCs by co-transplanting 100 CD34−CD135−KSL cells from WT or KO mice with 5×10^5 BJ competitor MNCs into lethally irradiated B6/BJ-F1 mice (Figure 3B). Chimerism from transplanted KO LT-HSCs gradually increased to 45.6% ± 19.5% at 4 months after transplantation relative to a significantly lower level of chimerism supported by WT-HSCs (4.85% ± 3.2%, P < .01, Figure 3B). Interestingly, data from secondary transplantation documented that at 12 weeks, chimerism in recipients of KO BM cells was not only significantly higher than that observed in recipients of primary WT BM, but that the level of engraftment in secondary recipients was higher than that documented in primary recipients. This can be easily explained by phenotypic analysis of BM from primary recipients 4 months after transplantation (Figure 3C). BM of mice receiving grafts from KO mice had a more than 4-fold higher frequency of KSL cells and in excess of 30-fold higher frequency of slamKSL cells (Figure 3C). These data demonstrate that LT-HSCs from Dmtf1-KO mice have higher self-renewal capabilities than their WT counterparts. Lineage reconstitution in the PB of primary recipients (supplemental Figure 2) mirrored the distribution in steady-state KO and WT mice, and the former had smaller T-cell pools (thymocytes and mature T cells) and larger B-cell

pools compared with the latter. Distribution of T/B/myeloid cells in mice transplanted with LT-HSCs showed similar results (data not shown).

Accelerated cell cycling of Dmtf1-KO BM under stress

Dmtf1 is a key molecule linking Raf/Erk oncogenic signaling and the Arf/Mdm2/p53 tumor-suppressor pathway,[23] and is implicated in the suppression of proliferation induced by proliferative and oncogenic signals. We therefore examined the impact of the loss of Dmtf1 on hematopoiesis in stress conditions induced by a genotoxic insult on BM cells. WT and Dmtf1-KO mice were treated with 5-FU and hematopoietic recovery was tracked over the next 25 days. Loss of Dmtf1 altered both the decline of circulating WBC counts early after 5-FU treatment (day 4) and recovery of these cells on day 11 and beyond (Figure 4A). On day 14 after treatment, rebound of WBC counts in KO mice was significantly higher than that in WT mice (270.1% ± 76.8% vs 151.2% ± 25.6%, respectively, Figure 4A). The lower WBC counts observed on day 4 in KO mice (54.2% vs 79.5%, respectively, P < .01) suggest that these BM cells have a higher frequency of cycling cells mainly because of the loss of the antiproliferation activity of Dmtf1. Using both Hst/Py staining and BrdU incorporation, we evaluated the cycling status of HSC-enriched fractions at day 5 after 5-FU. Because the expression of c-Kit is markedly diminished after 5-FU treatment,[33]
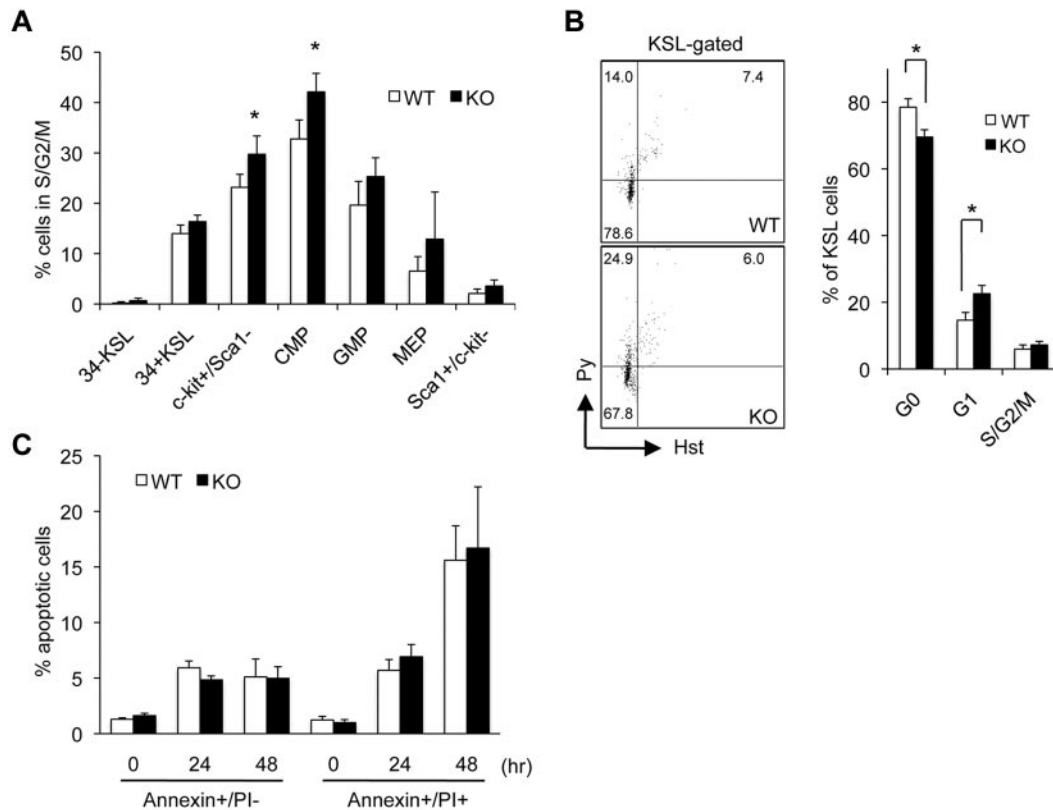
Figure 2. Cell-cycle alterations in steady-state BM of *Dmtf1*^{−/−} mice. (A) Cell-cycle analysis in steady-state BM was performed with DAPI. Percentages of cycling cells (S/G$_2$/M) are shown for each fraction (n = 4). *$P <$ .05. (B) Cell-cycle status of KSL cells was evaluated with Hst/Py staining. WT or *Dmtf1*^{−/−} BM low-density cells were stained for surface antigens followed by Hst/Py staining. Dot plots in panel B show representative results of Hst/Py staining of WT and KO cells depicting G$_0$ (bottom left quadrant), G$_1$ (top left quadrant), and S/G$_2$/M (top right quadrant) in KSL cells. Bar graph to the right shows the percentage of cells in the 3 phases of cell-cycle as average ± SD. *$P <$ .03. (C) Lin$^−$ cells from WT and *Dmtf1*^{−/−} mice were cultured without cytokines in serum-supplemented medium for the indicated times and stained with annexin V/propidium iodide (PI). Data shown are the mean percentage ± SD of annexin V$^+$/PI$^−$ and annexin V$^+$/PI$^+$ cells. No significant differences were observed between WT and *Dmtf1*^{−/−} mice (n = 3).

we analyzed total Lin$^−$Sca1$^+$ cells with c-Kit$^{+/dim}$ expression (Figure 4B). A significantly lower fraction of KSL cells from KO mice were in G$_0$, whereas a substantially higher percentage of these cells were in S/G$_2$ + M (Figure 4B). To focus on more primitive cells, we next examined BrdU incorporation in slamKSL cells (Figure 4C). Whereas only 6.2% ± 1.0% of slamKSL cells from WT mice were BrdU$^+$, almost a 2-fold increase in the number of BrdU$^+$ slamKSL cells was detected in KO mice (11.1% ± 1.9%). Interestingly, in steady-state hematopoiesis (supplemental Figure 3), WT and KO mice contained similar frequencies of slamKSL cells that were BrdU$^+$ after a short (2-hour) pulse (1.8% ± 0.6% for WT mice and 1.9% ± 0.8% for KO mice). To further assess the ability of Dmtf1 BM cells to support hematopoiesis under stress conditions, we examined the survival of mice serially treated with 5-FU, a treatment that leads to hyperproliferation and exhaustion of stem cells.[5] To evaluate HSC-intrinsic factors only, we examined recipients that had been transplanted with KO or WT BM cells 3 months previously. Mice reconstituted with either WT or KO cells succumbed at the same rate to hematopoietic exhaustion and had no statistically significant differences in survival (Figure 4D). These data suggest that *Dmtf1*-KO BM cells are more mitotically active than WT cells, especially under conditions of hematopoietic stress, and illustrate that *Dmtf1*-deficient HSCs have a higher repopulating capacity without premature exhaustion.

Dysregulation of cdkn1a (p21) and Arf in *Dmtf1*-null HSCs

It has been reported previously that Arf is not expressed in steady-state KSL cells, but is induced upon in vitro cytokine stimulation. We evaluated the regulation of Arf and cdkn1a (p21) in *Dmtf1*-KO HSCs

during cytokine stimulation in vitro. As described previously,[9] freshly isolated WT KSL cells did not express Arf (Figure 5A). Arf expression in these cells was not detected until after 72 hours in culture (Figure 5A). However, *Dmtf1*-KO KSL cells did not express Arf at any time point, including 72 hours after culture initiation, and showed markedly suppressed expression of cdkn1a (p21) throughout culture (Figure 5A). Because Arf induction may reduce HSC function,[10] we examined whether dysregulation of cdkn1a (p21) and Arf may contribute to enhanced repopulating capacity of cultured *Dmtf1*-KO HSCs. KSL cells from WT or KO mice cultured with cytokines for 72 hours were transplanted competitively into irradiated B6/BJ-F1 mice. Chimerism at 1 month after transplantation was modestly higher in mice that received cultured KO KSL cells compared with recipients of WT KSL cells (24.5% ± 6.0% vs 16.7% ± 4.0%, respectively, $P =$ .05, Figure 5B). However, donor-derived chimerism in mice transplanted with cultured KO KSL cells increased at 4 months after transplantation, whereas that in recipients of cultured WT KSL cells declined with time (30.6% ± 9.4% vs 13.7% ± 6.5%, respectively, $P =$ .03, Figure 5B). Interestingly, the BM of mice receiving cultured KO KSL cells contained a more than 10-fold higher frequency of KSL cells than the BM of WT KSL recipients (supplemental Figure 4). These data strongly suggest that *Dmtf1*-KO HSCs preserve their self-renewal capacity in cytokine-induced stress conditions, most likely because these cells fail to express Arf.

Dmtf1 functions in Arf-dependent and Arf-independent pathways

Although Dmtf1 KSL cells show altered regulation of Arf and cdkn1a (p21), both molecules are believed to have a limited impact on HSC
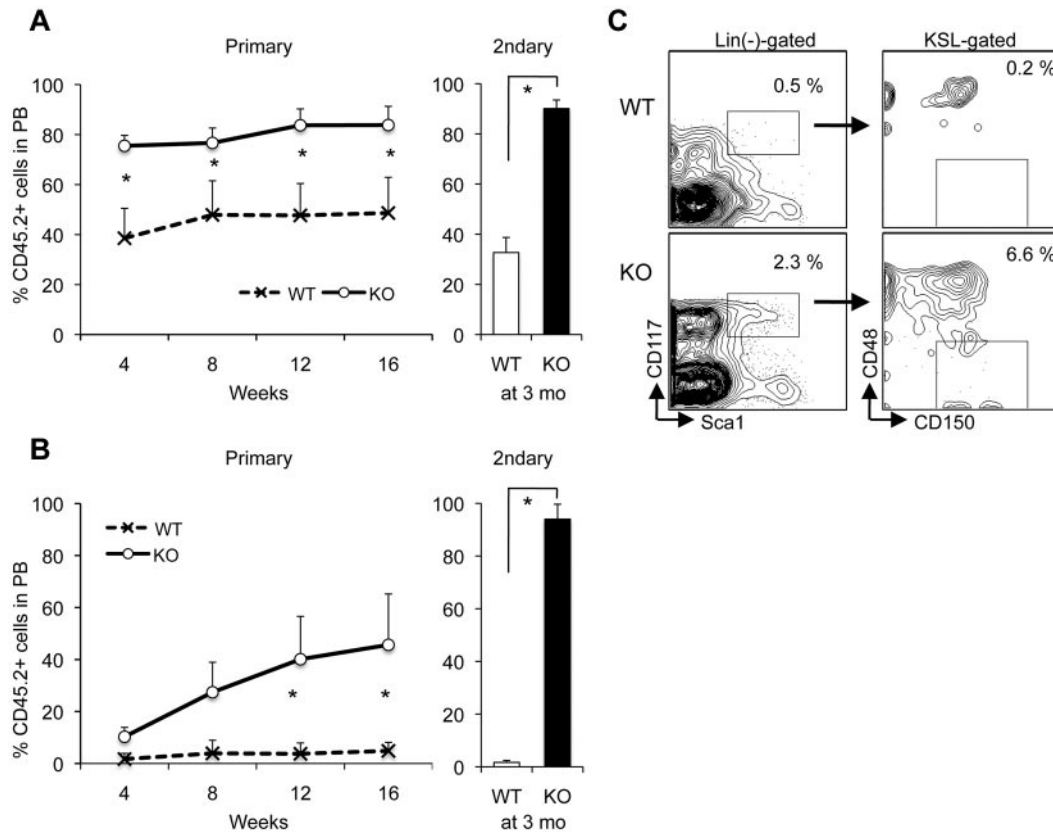
Figure 3. Enhanced long-term reconstitution capacity of LT-HSCs from *Dmtf1*⁻/⁻ mice. Recipient mice were transplanted with 2×10^5 BM-MNCs from WT or KO mice (CD45.2⁺) and an equal number of BM-MNCs from BJ mice (CD45.1⁺; A) or 100 CD34-135-KSL cells from *Dmtf1*⁺/⁺ or *Dmtf1*⁻/⁻ mice plus 5×10^5 competitor MNCs from BJ mice to reconstitute lethally irradiated B6/BJ-F1 recipients (CD45.2 + 45.1⁺; B). Chimerism was assessed monthly. Data shown are the mean chimerism shown as percentage ± SD of donor-derived cells in PB (n = 4 per group per experiment). **$P < .05$. Next to panels A and B in bar graphs are the results of secondary transplants in which each secondary recipient received 2×10^5 BM-MNCs from a primary recipient 4 months after the primary transplantation. Data analysis in secondary recipients was performed 4 months after transplantation. (C) One representative dot plot of CD48/150 distribution in the KSL fraction of primary recipient BM at 4 months after transplantation with LT-HSCs from KO or WT mice.

function.[3,9] We examined the role of Dmtf1 in Arf signaling in HSCs. We generated 2 retroviral vector constructs (supplemental Figure 5A) with a FL form (MIEG-FL) and a DN form (MIEG-DN) of human Dmtf1 (hDmtf1) and transduced Jurkat T cells with a homozygous deletion of the *Arf/Ink4a* locus. We confirmed that neither hDmtf1 nor hArf was expressed in Jurkat cells (supplemental Figure 5B). GFP-sorted Jurkat-FL showed a lower frequency of cycling cells compared with Jurkat-DN (Figure 6A), and therefore, Jurkat-DN cells had a higher proliferative potential than Jurkat-FL cells (Figure 6B), suggesting that Dmtf1 can be functional in *Arf*-null cells. We next examined the effect of Arf expression in *Dmtf1*-null cells. The retroviral vectors MIG-Mock and MIG-Arf (supplemental Figure 5A) were transduced into BM Lin⁻ cells, followed by purification by GFP sorting and evaluation of hematopoietic potential by clonogenic assays. MIG-Mock–transduced Lin⁻ cells from KO mice (Mock/KO) produced a significantly higher number of colonies compared with similarly transduced cells from WT mice (Figure 6C). Although introduction of Arf induced a decline in the clonogenic potentials of both WT and KO Lin⁻ cells (Arf/WT and Arf/KO, respectively), Arf/KO cells maintained higher numbers of clonogenic cells compared with Arf/WT as a result of partial suppression (Figure 6C). These data suggest that Dmtf1 can induce a negative regulation of cell-cycle progression via both Arf-independent and Arf-dependent pathways. To examine this more fully, we investigated candidate molecules that may contribute to the Dmtf1-mediated regulation of the cell cycle. Using quantitative RT-PCR of sorted KSL cells from WT and KO mice, we quantified the expression of multiple cell cycle–related genes. Reductions in the expression of cdkn1c (p57) and

CCND1 and an increase in the expression of CDK6 were detected in KO KSL cells (Figure 6D). No statistical differences in the expression of CDKN1b (p27) and CDKN2c (p18) were detected (Figure 6D). We also examined the Jun family transcription factors, which can be candidate targets for Dmtf1. Expression of JunB, which is heavily implicated in tumor suppression, was markedly decreased in KSL cells from KO mice, a trend that was not observed for C-Jun and Bmi1 (Figure 6D). Suppression of JunB expression was also observed in B cells and CD4⁺ T cells from KO mice (Figure 6E). These data suggest a possible involvement of JunB in Dmtf1 signaling. Because stem-cell function in KO mice was not exhausted, it was important to examine the status of p57 and p27 in long-term repopulating cells from KO mice to confirm that these CDK2 inhibitors were not suppressed in KO mice. As expected from the functional behavior of long-term repopulating cells from KO mice, data shown in Figure 7 demonstrate that expression of neither CDKN1C (p57) nor CDKN1b (p27) was significantly reduced in KO long-term repopulating cells relative to those from WT mice, and that only p57 expression in KO short-term repopulating cells and MPP was reduced.

Discussion

It is well established that Ras/Raf/ERK signaling plays a central role in growth factor–mediated proliferation, differentiation, oncogenesis, and apoptosis of a variety of cells. In addition, p53 is a critical regulator protecting cells from multiple forms of stress
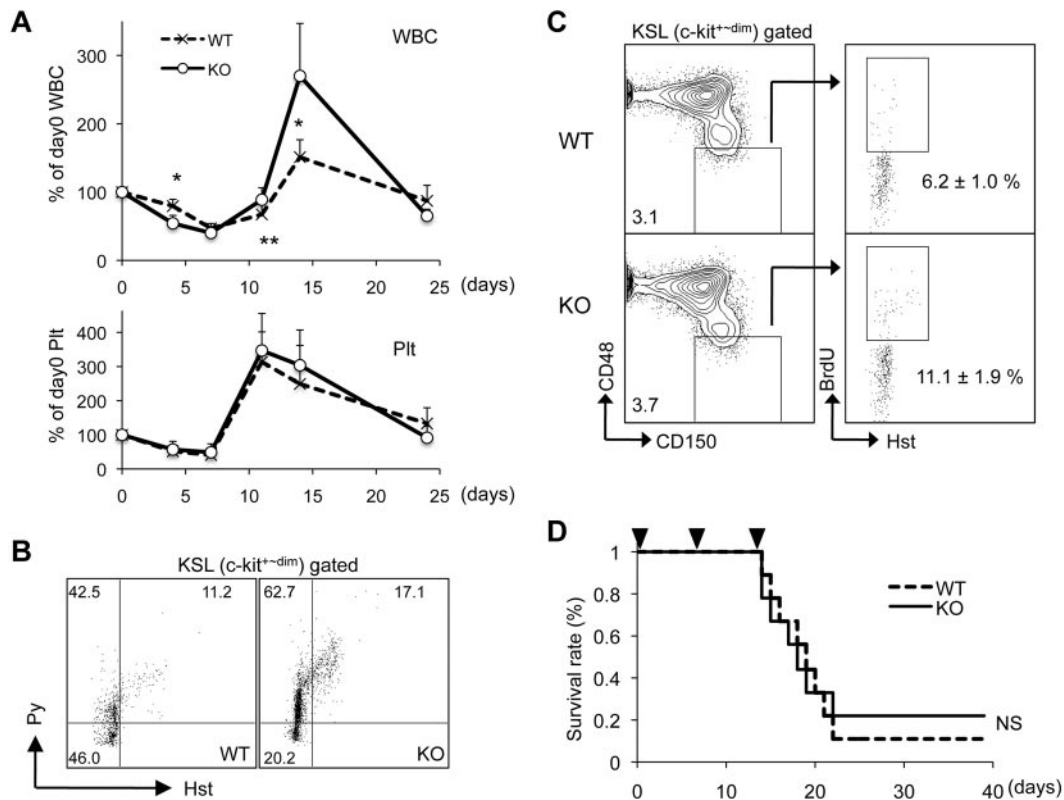
Figure 4. $Dmtf1^{-/-}$ BM cells have enhanced rebound kinetics after myelotoxic stress. (A) Kinetics of PB count during recovery from BM suppression after a single injection of 5-FU (150 mg/kg; n = 7-8 per genotype). (B) BM cells from WT or $Dmtf1$-KO mice were collected 5 days after a single injection of 5-FU (150 mg/kg) and were stained with Hst/Py. One representative set of dot plots from 3 independent experiments with similar results showing cell-cycle status of WT and KO KSL cells. (C) BrdU incorporation in slamKSL cells at day 5 after a single injection of 5-FU (150 mg/kg). Results are shown as average ± SD (n = 3). *P < .03. (D) $Dmtf1^{+/+}$ or $Dmtf1^{-/-}$ BM cells were transplanted into irradiated B/J mice (n = 10 for each group). After 3 months, 5-FU (135 mg/kg) was injected IP weekly for 3 consecutive weeks and survival was monitored daily. Data shown were plotted in a Kaplan-Meyer curve and the results were analyzed with a log-rank nonparametric test.

signals. Dmtf1 is emerging as a novel key molecule linking Ras/Raf/ERK growth-promoting signaling and the Arf/p53/p21 tumor-suppressor pathway.[23] The goal of the present study was to determine whether Dmtf1 affects HSC self-renewal and differentiation through the modulation of cell-cycle regulation. Using different in vivo and in vitro assays, we have shown that HSC quiescence is altered in the absence of Dmtf1.

The h$Dmtf1$1 locus was lost in leukemic cells with chromosome 7q abnormalities regardless of the detailed karyotype.[28] In addition, $Dmtf1$ is deleted in approximately 40% of mouse models of lung cancers, and the h$Dmtf1$ deletion can be demonstrated in approximately 35% of human lung cancer cells, particularly when the Arf and/or p53 locus is retained.[27] These observations suggest that Dmtf1 is a physiologic regulator of the Arf/p53 pathway, whereas in some cases, it imparts a growth-suppression effect in $p53$-deficient lung cancer cells.[27] Based on these findings, we hypothesized that Dmtf1 may play a role in HSC self-renewal similar to the previously reported involvement of $p53$ in HSC quiescence.[20] Indeed, when we examined $Dmtf1$-KO mice, we observed higher levels of circulating MNCs, and when HSC from these mice were used in transplantation studies, higher levels of chimerism were sustained in recipient mice. This demonstrates similar functional properties between HSCs from $Dmtf1$-KO mice and cells from p53-null mice.

Based on known functions of Dmtf1, we anticipated that it might play a more critical role in the regulation of the cell cycle under stress conditions rather than steady-state hematopoiesis. Analysis of steady-state Kit$^+$ and KSL cells from KO and WT mice revealed only minor differences in cell-cycle status (Figure 2). However, under 5-FU–induced stress, the cycling status of BM

cells from KO mice was higher than that of cells from WT mice, as evidenced by lower PB counts on day 4 after 5-FU treatment (Figure 4A), with a higher percentage of cells in G_1 or $S/G_2/M$ on day 5 after 5-FU treatment (Figure 4B). We analyzed slamKSL cells for BrdU incorporation into HSCs because these cells have been used before as positive indicators of HSCs after cytotoxic/G-CSF treatment.[34] Although the frequency of slamKSL cells between $Dmtf1$-KO and WT mice was similar (data not shown), the percentage of BrdU$^+$ slamKSL cells was 2-fold higher in Dmtf1 KO BM, suggesting that Dmtf1 negatively regulates HSC cell-cycle progression under stress conditions.

As a tumor suppressor, Dmtf1 is haploinsufficient, and therefore behaves as many other bona fide TSGs, including Rb, neurofibromatosis 1 ($NF1$), and $p53$.[8] Interestingly, we observed enhanced in vitro hematopoietic activity (Figure 1A-B). Comparable levels of chimerism were observed when mice were transplanted with BM cells from $Dmtf1^{+/-}$ or $Dmtf1^{-/-}$ mice, and $Dmtf1^{+/-}$ mice showed similar hematopoietic recovery as KO mice after 5-FU treatment (data not shown). These data are in full agreement with those of Inoue et al demonstrating that haploinsufficiency of Dmtf1 suppresses cell growth.[25]

CDK inhibitors can be divided into 2 groups: the Ink4 proteins (p16, p15, p18, and p19), which inhibit CDK4/6, and the Cip/Kip proteins (p21, p27, and p57), which inhibit CDK2. CDK4/6 might be important for self-renewal divisions, because the absence of INK4 inhibitors generally leads to enhanced HSC engraftment, whereas deletion of CDK2 inhibitors is associated with stem-cell exhaustion. Although the expression/induction of cdkn1a (p21) was impaired in $Dmtf1^{-/-}$ KSL cells (Figure 5A), its impact on regulation of $Dmtf1^{-/-}$ HSCs is probably minimal given the limited

Figure 5. Dysregulation of CDKN1a (p21) and Arf in *Dmtf1*$^{-/-}$ KSL cells. (A) Sorted KSL cells from null or WT mice were cultured with SCF/TPO/Flt3-ligand/IL-3. Cells were harvested at the indicated time points and the expression of cdkn1a (p21) and Arf were evaluated by quantitative RT-PCR. (B) One thousand sorted KSL cells from KO or WT mice were cultured for 72 hours under the same conditions described in panel A, and then transplanted into lethally irradiated mice in competition with 3×10^5 B/J MNCs. Chimerism was analyzed by flow cytometric analysis (n = 5 in each group).
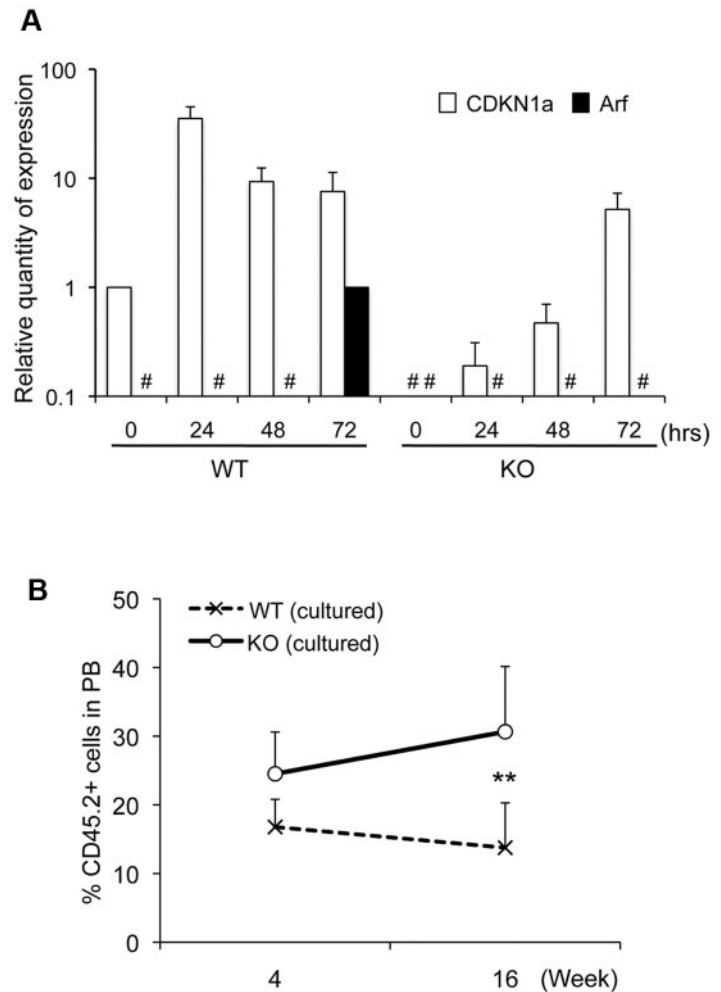
role of cdkn1a (p21) in normal HSC function[3] and its requirement in maintaining leukemic stem cells.[3,4]

The effects of Arf on HSC regulation remain controversial. Arf was not expressed in steady-state KSL from Arf-GFP reporter mice, and was induced in only a fraction of KSL cells after in vitro culture with cytokines,[9] as we demonstrated in our studies (Figure 5A). In addition, *Arf*-deficient HSCs did not display obvious alterations in their BM-repopulating potential,[9] suggesting that Arf does not affect HSC function. Conversely, *Bmi*-null HSCs have a critical self-renewal impairment associated with marked up-regulation of Arf/Ink4a; indeed, the impaired self-renewal capacity in these cells is dramatically compensated for by Arf/Ink4a disruption.[10] In addition, Arf is induced by not only growth-promoting stimulation, but also by other stress conditions including oxidative stress[35] and irradiation.[36] These observations suggest that Arf plays a role in the regulation of HSCs under certain stress conditions. Whereas Stepanova and Sorrentino[9] examined the repopulating potential of HSCs cultured for 12 days, we examined the in vivo functional capacity of HSCs cultured for 3 days only, because self-renewal of HSCs was conserved within 72 hours of culture.[37] Chimerism sustained by KO KSL cells at 4 months after transplantation was higher than that observed with WT cells (Figure 5B), suggesting that suppression of Arf induction in cultured KO KSL cells may contribute to the conservation of self-renewal potential. These data corroborate our hypothesis that

Arf plays an important role in HSC regulation in stress but not steady-state hematopoiesis.

We also examined whether Dmtf1 signaling was dependent on Arf. We used Jurkat T cells, which have a genetic deletion of the *Arf/Ink4a* locus, and observed that cells transduced with hDmtf1-FL showed a lower frequency of cycling cells and slower proliferation kinetics than cells transduced with hDmtf1-DN (Figure 6B), suggesting an Arf-independent Dmtf1 signaling pathway, as was previously suggested by Inoue et al in hematopoietic cells.[29] In contrast, when Arf was overexpressed in *Dmtf1* KO or WT BM progenitor cells, we observed both an Arf-dependent and an Arf-independent pathway for regulation of proliferation (Figure 6C). To examine the Arf-independent pathway, we investigated the expression of many CDK-related molecules and Jun-family genes. Quantitative RT-PCR analysis revealed that whereas several transcripts were down-regulated, CDK6 was up-regulated in KSL cells from KO mice. Interestingly, the induction of CDK6 enhances the proliferation of normal myeloid progenitors,[38] suggesting that increased CDK6 expression may contribute to the phenotype of *Dmtf1*-KO mice. This was further supported by the finding that p57 and p27 were not suppressed in LT-HSCs from KO mice, lending further corroboration to the observed enhanced repopulating potential of HSCs from these mice. JunB, along with c-Jun and JunD, forms homodimers or heterodimers with members of the Fos family protein, resulting in the activation of transcription factor proteins. It has been shown that JunB has important roles as a tumor suppressor in hematopoiesis for not only
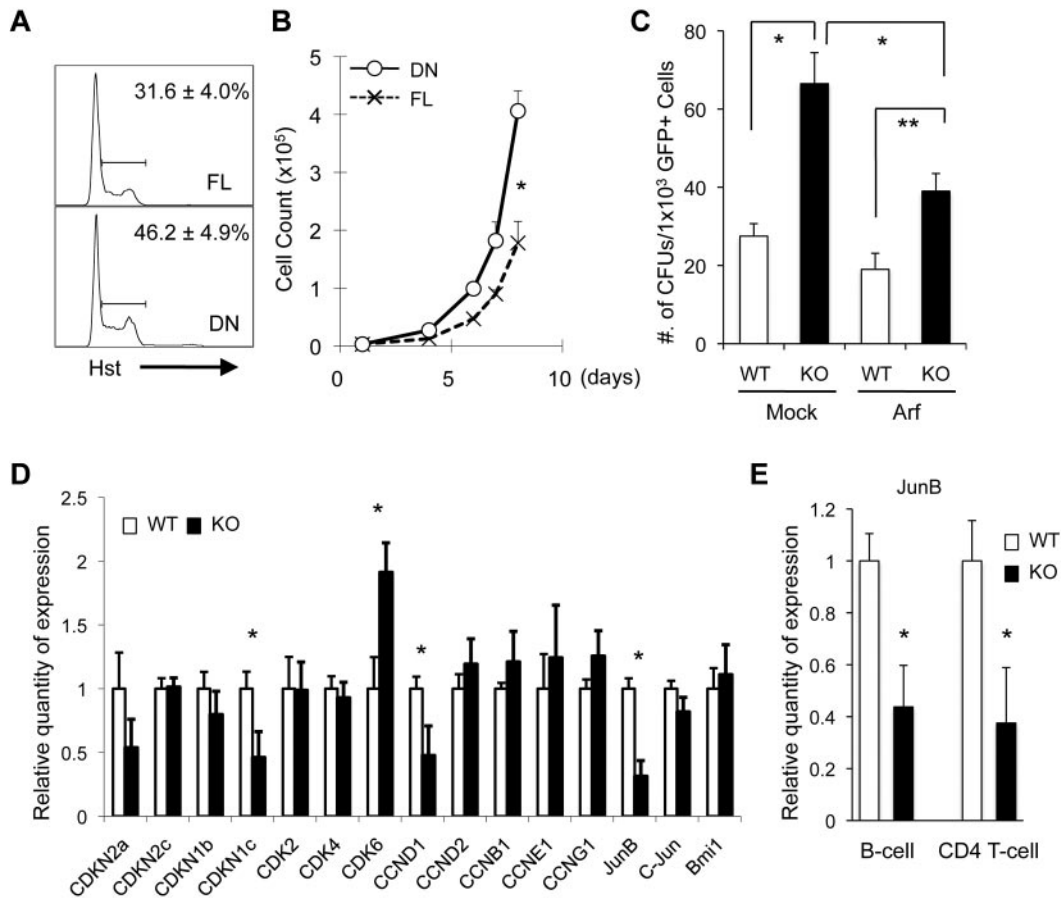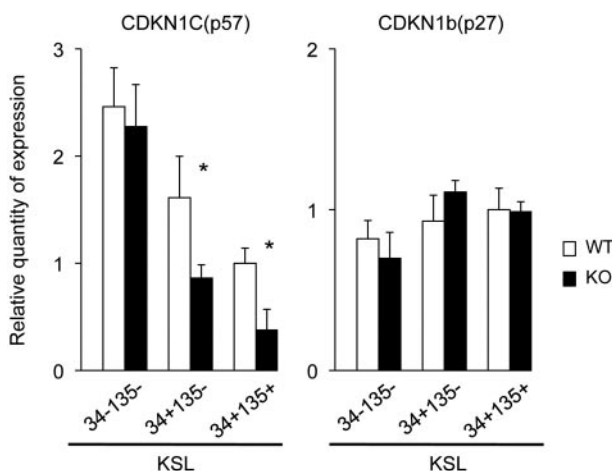
Figure 6. Dmtf1 has both Arf-dependent and Arf-independent pathways. (A) Human Dmtf1-FL or Dmtf1-DN were retrovirally transduced into Jurkat T cells (*Arf*-null) and purified by GFP sorting. Cell-cycle analysis was measured with Hst staining. Results are shown as average ± SD (n = 3). *P < .05. (B) Cell numbers of Jurkat cells expressing FL or DN were determined daily. *P < .01. Results shown are from 1 of 3 independent experiments. (C) Retroviral vector MIG-Arf and MIG-Mock were transduced into WT or *Dmtf1*-KO Lin⁻ cells, and GFP⁺ cells were sorted flow cytometrically and used in a CFU assay. Results are from 1 of 3 independent experiments. *P < .01 and **P < .03. (D) Analysis of gene expression in *Dmtf1*-KO KSLs by quantitative RT-PCR analysis of RNA isolated from sorted KSL cells from primary *Dmtf1*-KO or WT. The relative expression is shown normalized to gene expression in control HSCs (mean ± SD, n = 3). *P < .05. (E) Relative expressions of JunB in B and CD4⁺ T cells. Sorted splenic B cells and CD4⁺ T cells were analyzed by quantitative RT-PCR. The relative expression is shown normalized to gene expression in WT CD4 or B cells, respectively (mean ± SD, n = 3). *P < .05.

protecting against myeloid malignancies,[39] but also for inhibiting proliferation and transformation of B-lymphoid cells.[40] However, the role of JunB in T-lymphoid cells is unclear. In fact, JunB is rarely

Figure 7. Expression of CDKN1C (p57) and CDKN1b (p27). Gene expression of CDKN1C (p57) and CDKN1b (p27) in the LT-HSC compartment was measured with quantitative RT-PCR analysis. RNAs were isolated from sorted LT-HSCs, ST-HSCs, and MPP cells from primary *Dmtf1*-KO or WT mice. Relative expressions are shown normalized to gene expression in WT MPP cells (mean ± SD, n = 3). *P < .05.

expressed or missing in B-cell malignancies despite the up-regulated expression in T-cell malignancies.[41,42] A recent study implicated JunB as one of the targets of Dmtf1, showing that its expression was decreased in lung cells from *Dmtf1*-KO mice.[43] We therefore predicted reduced JunB expression in sorted KSL cells, B cells, and CD4 T cells from KO mice relative to similar WT cells (Figure 6) and increased B-cell populations with reciprocal T-cell reductions in both primary KO mice and mice transplanted with KO BM cells (Table 1 and supplemental Figure 2). These findings are consistent with previous observations about distinctive JunB function in T and B cells, suggesting that JunB is potentially involved in a Dmtf1-mediated, Arf-independent pathway. Additional studies aimed at examining the regulation of JunB by Dmtf1 are warranted. Interestingly, because Bmi1 is involved in the regulation of Arf, we also examined whether changes in JunB expression on KSL cells is also associated with changes in Bmi1 expression (Figure 6D). Our data did not reflect any changes in the expression of Bmi1 on KSL cells, suggesting that, most likely, Bmi1 does not change JunB expression.

These studies shed additional light on the mechanisms involved in the maintenance of HSC quiescence and proliferation in stress and steady-state hematopoiesis, and underscore the role of Dmtf1 as a modulator of these HSC properties. In addition, our studies begin to explain how Dmtf1, which is disrupted in many cancer cells, contributes to HSC maintenance, suggesting its possible use as a target for new therapeutic strategies in cancer.

Authorship

Contribution: M.K. performed all of the research and assisted in the experimental design and writing the manuscript; and E.F.S. assisted in the experimental design, data interpretation, and writing the manuscript.

Conflict-of-interest disclosure: The authors declare no competing financial interests.

Correspondence: Edward F. Srour, PhD, Robert J. and Annie S. Rohn Professor of Leukemia Research, Professor of Medicine, Indiana University School of Medicine, 980 W Walnut St, R3-C312, Indianapolis, IN 46202; e-mail: esrour@iupui.edu.

References

1. Wilson A, Trumpp A. Bone-marrow haematopoietic-stem-cell niches. *Nat Rev Immunol.* 2006; 6(2):93-106.

2. Cheng T, Rodrigues N, Shen H, et al. Hematopoietic stem cell quiescence maintained by p21cip1/waf1. *Science.* 2000;287(5459):1804-1808.

3. van Os R, Kamminga LM, Ausema A, et al. A Limited role for p21Cip1/Waf1 in maintaining normal hematopoietic stem cell functioning. *Stem Cells.* 2007;25(4):836-843.

4. Viale A, De Franco F, Orleth A, et al. Cell-cycle restriction limits DNA damage and maintains self-renewal of leukaemia stem cells. *Nature.* 2009; 457(7225):51-56.

5. Cheng T, Rodrigues N, Dombkowski D, Stier S, Scadden DT. Stem cell repopulation efficiency but not pool size is governed by p27(kip1). *Nature Medicine.* 2000;6(11):1235-1240.

6. Rosu-Myles M, Taylor BJ, Wolff L. Loss of the tumor suppressor p15Ink4b enhances myeloid progenitor formation from common myeloid progenitors. *Exp Hematol.* 2007;35(3):394-406.

7. Yuan Y, Shen H, Franklin DS, Scadden DT, Cheng T. In vivo self-renewing divisions of haematopoietic stem cells are increased in the absence of the early G1-phase inhibitor, p18(INK4C). *Nat Cell Biol.* 2004;6(5):436-442.

8. Sherr CJ. Principles of tumor suppression. *Cell.* 2004;116(2):235-246.

9. Stepanova L, Sorrentino BP. A limited role for p16Ink4a and p19Arf in the loss of hematopoietic stem cells during proliferative stress. *Blood.* 2005;106(3):827-832.

10. Oguro H, Iwama A, Morita Y, Kamijo T, van Lohuizen M, Nakauchi H. Differential impact of Ink4a and Arf on hematopoietic stem cells and their bone marrow microenvironment in Bmi1-deficient mice. *J Exp Med.* 2006;203(10):2247-2253.

11. Zhang J, Grindley JC, Yin T, et al. PTEN maintains haematopoietic stem cells and acts in lineage choice and leukaemia prevention. *Nature.* 2006;441(7092):518-522.

12. Qian Z, Chen L, Fernald AA, Williams BO, Le Beau MM. A critical role for Apc in hematopoietic stem and progenitor cell survival. *J Exp Med.* 2008;205(9):2163-2175.

13. Akala OO, Park IK, Qian D, Pihalja M, Becker MW, Clarke MF. Long-term haematopoietic reconstitution by Trp53−/−p16Ink4a−/−p19Arf−/− multipotent progenitors. *Nature.* 2008;453(7192):228-232.

14. Chen J, Ellison FM, Keyvanfar K, et al. Enrichment of hematopoietic stem cells with SLAM and LSK markers for the detection of hematopoietic stem cell function in normal and Trp53 null mice. *Exp Hematol.* 2008;36(10):1236-1243.

15. TeKippe M, Harrison DE, Chen J. Expansion of

hematopoietic stem cell phenotype and activity in Trp53-null mice. *Exp Hematol.* 2003;31(6):521-527.

16. Wlodarski P, Wasik M, Ratajczak MZ, et al. Role of p53 in hematopoietic recovery after cytotoxic treatment. *Blood.* 1998;91(8):2998-3006.

17. Dumble M, Moore L, Chambers SM, et al. The impact of altered p53 dosage on hematopoietic stem cell dynamics during aging. *Blood.* 2007; 109(4):1736-1742.

18. Lotem J, Sachs L. Hematopoietic cells from mice deficient in wild-type p53 are more resistant to induction of apoptosis by some agents. *Blood.* 1993;82(4):1092-1096.

19. Park IK, Qian D, Kiel M, et al. Bmi-1 is required for maintenance of adult self-renewing haematopoietic stem cells. *Nature.* 2003;423(6937):302-305.

20. Liu Y, Elf SE, Miyata Y, et al. p53 regulates hematopoietic stem cell quiescence. *Cell Stem Cell.* 2009;4(1):37-48.

21. Inoue K, Sherr CJ. Gene expression and cell cycle arrest mediated by transcription factor DMP1 is antagonized by D-type cyclins through a cyclin-dependent-kinase-independent mechanism. *Mol Cell Biol.* 1998;18(3):1590-1600.

22. Inoue K, Wen R, Rehg JE, et al. Disruption of the ARF transcriptional activator DMP1 facilitates cell immortalization, Ras transformation, and tumorigenesis. *Genes Dev.* 2000;14(14):1797-1809.

23. Sreeramaneni R, Chaudhry A, McMahon M, Sherr CJ, Inoue K. Ras-Raf-Arf signaling critically depends on the Dmp1 transcription factor. *Mol Cell Biol.* 2005;25(1):220-232.

24. Inoue K, Roussel MF, Sherr CJ. Induction of ARF tumor suppressor gene expression and cell cycle arrest by transcription factor DMP1. *Proc Natl Acad Sci U S A.* 1999;96(7):3993-3998.

25. Inoue K, Zindy F, Randle DH, Rehg JE, Sherr CJ. Dmp1 is haplo-insufficient for tumor suppression and modifies the frequencies of Arf and p53 mutations in Myc-induced lymphomas. *Genes Dev.* 2001;15(22):2934-2939.

26. Inoue K, Sugiyama T, Taneja P, Morgan RL, Frazier DP. Emerging roles of DMP1 in lung cancer. *Cancer Res.* 2008;68(12):4487-4490.

27. Mallakin A, Sugiyama T, Taneja P, et al. Mutually exclusive inactivation of DMP1 and ARF/p53 in lung cancer. *Cancer Cell.* 2007;12(4):381-394.

28. Bodner SM, Naeve CW, Rakestraw KM, et al. Cloning and chromosomal localization of the gene encoding human cyclin D-binding Myb-like protein (hDMP1). *Gene.* 1999;229(1-2):223-228.

29. Inoue K, Mallakin A, Frazier DP. Dmp1 and tumor suppression. *Oncogene.* 2007;26(30):4329-4335.

30. Fukuda S, Mantel CR, Pelus LM. Survivin regulates hematopoietic progenitor cell proliferation through

p21WAF1/Cip1-dependent and -independent pathways. *Blood.* 2004;103(1):120-127.

31. Wilson A, Laurenti E, Oser G, et al. Hematopoietic stem cells reversibly switch from dormancy to self-renewal during homeostasis and repair. *Cell.* 2008;135(6):1118-1129.

32. Taneja P, Mallakin A, Matise LA, Frazier DP, Choudhary M, Inoue K. Repression of Dmp1 and Arf transcription by anthracyclins: critical roles of the NF-kappaB subunit p65. *Oncogene.* 2007; 26(53):7457-7466.

33. Randall TD, Weissman IL. Phenotypic and functional changes induced at the clonal level in hematopoietic stem cells after 5-fluorouracil treatment. *Blood.* 1997;89(10):3596-3606.

34. Yilmaz OH, Kiel MJ, Morrison SJ. SLAM family markers are conserved among hematopoietic stem cells from old and reconstituted mice and markedly increase their purity. *Blood.* 2006; 107(3):924-930.

35. Ito K, Hirao A, Arai F, et al. Reactive oxygen species act through p38 MAPK to limit the lifespan of hematopoietic stem cells. *Nat Med.* 2006;12(4): 446-451.

36. Wang Y, Schulte BA, LaRue AC, Ogawa M, Zhou D. Total body irradiation selectively induces murine hematopoietic stem cell senescence. *Blood.* 2006;107(1):358-366.

37. Nakauchi H, Sudo K, Ema H. Quantitative assessment of the stem cell self-renewal capacity. *Ann N Y Acad Sci.* 2001;938:18-24;discussion 24-15.

38. Fujimoto T, Anderson K, Jacobsen SE, Nishikawa SI, Nerlov C. Cdk6 blocks myeloid differentiation by interfering with Runx1 DNA binding and Runx1-C/EBPalpha interaction. *EMBO J.* 2007;26(9):2361-2370.

39. Passegué E, Wagner EF, Weissman IL. JunB deficiency leads to a myeloproliferative disorder arising from hematopoietic stem cells. *Cell.* 2004; 119(3):431-443.

40. Szremska AP, Kenner L, Weisz E, et al. JunB inhibits proliferation and transformation in B-lymphoid cells. *Blood.* 2003;102(12):4159-4165.

41. Mao X, Orchard G, Lillington DM, Russell-Jones R, Young BD, Whittaker SJ. Amplification and overexpression of JUNB is associated with primary cutaneous T-cell lymphomas. *Blood.* 2003; 101(4):1513-1519.

42. Rassidakis GZ, Thomaides A, Atwell C, et al. JunB expression is a common feature of CD30+ lymphomas and lymphomatoid papulosis. *Mod Pathol.* 2005;18(10):1365-1370.

43. Mallakin A, Sugiyama T, Kai F, et al. The Arf-inducing transcription factor Dmp1 encodes a transcriptional activator of amphiregulin, thrombospondin-1, JunB and Egr1. *Int J Cancer.* 2010; 126(6):1403-1416.